Journal of Molecular Structure 970 (2010) 42–50

Contents lists available at ScienceDirect

Journal of Molecular Structure

journal homepage: www.elsevier.com/locate/molstruc

Synthesis, structure and conformational analysis of 2,4-diaryl-3-azabicyclo[3.3.1]nonan-9-one thiosemicarbazones and semicarbazones

R. Ramachandran, M. Rani, S. Kabilan *

Department of Chemistry, Annamalai University, Annamalainagar 608002, Tamil Nadu, India

ARTICLE INFO

Article history:
Received 12 November 2009
Received in revised form 31 January 2010
Accepted 1 February 2010
Available online 6 February 2010

Keywords:
2,4-Diaryl-3-azabicyclo[3.3.1]nonan-9-one
^{1}H–^{1}H COSY
NOESY
Conformational study
Crystal structure

ABSTRACT

A series of thiosemicarbazones and semicarbazones have been synthesized and characterized by one and two dimensional NMR spectroscopy. The possible ring conformations of both the hydrazones are discussed. The chemical shifts and coupling constants suggest that the reported hydrazones adopt twin-chair conformations with equatorial orientation of the aryl substituents. Besides, the proposed conformations are further confirmed by single crystal X-ray diffraction analysis and molecular optimization geometry method.

Crown Copyright © 2010 Published by Elsevier B.V. All rights reserved.

1. Introduction

Hydrazones are of considerable pharmacological interest since a number of derivatives have shown whole panoply of chemotherapeutic properties [1]. Antimalarial activities of thiosemicarbazones and semicarbazones have been previously reported [2]. Indeed, many hydrazones exhibit promising anti-protozoan activity through the inhibition of cysteine proteases and other targets [3–6]. The hydrazones are also a member of class of metal-chelators that are Schiff bases. For example iron (Fe) is essential for the biological activity of a number of plasmodial proteins, including the rate-limiting enzyme of DNA synthesis, ribonucleotide reductase, withholding it inhibits the growth of the malaria parasite [7,8]. On the other hand, the bicyclic compounds occupy a special place in the structural elucidation, conformation and stereochemistry. In connection with our earlier work on spectral [9] studies of variously substituted mono and bicyclic compounds, herein we report the characterization of bicyclic thiosemicarbazones and semicarbazones using spectral and single crystal X-ray analysis.

2. Experimental

2.1. Physical measurements

The melting points were recorded in an open capillary tube and are uncorrected. IR spectra have been recorded in AVATAR-330 FT-IR spectrophotometer (Thermo Nicolet). For compounds S9, **S11**–**S23**, ^{1}H and ^{13}C NMR spectra have been recorded at 400 and 100 MHz, respectively on a BRUKER AMX 400 MHz spectrometer using $CDCl_3$ as solvent and TMS as internal standard. For compound **S10**, ^{1}H, ^{13}C and 2D NMR (HOMOCOSY and NOESY) spectra have been recorded on a BRUKER AMX 500 MHz spectrometer using $CDCl_3$ as solvent and TMS as internal reference, for which the operating frequency of ^{1}H is 500 MHz and ^{13}C is 125 MHz. All the spectra of compounds **S10**–**S23** were measured at a temperature of 300 K (chemical shift in δ ppm).

2.2. Synthesis of 2,4-diaryl-3-azabicyclo[3.3.1]nonan-9-one thiosemicarbazones (*S10*–*S17*)

To a boiling solution of 2,4-diaryl-3-azabicyclo[3.3.1]nonan-9-one (0.01 mol) in ethanolic chloroform (45 ml), the ethanolic chloroform solution of thiosemicarbazide hydrochloride (0.01 mol) was added drop wise with constant stirring. The reaction mixture was refluxed for 3 h on a water bath. After cooling the solid product was filtered off and purified by column chromatography.

2.3. Synthesis of 2,4-diaryl-3-azabicyclo[3.3.1]nonan-9-one semicarbazones (*S18*–*S23*)

To a boiling solution of bicyclic ketone (0.01 mol) in ethanolic chloroform (1:1), semicarbazide hydrochloride (0.012 mol) and sodium acetate trihydrate (0.03 mol) were added and refluxed for about 6 h. After the usual workup, the solid was separated and purified by column chromatography.

* Corresponding author. Tel.: +91 9443924629.
E-mail address: chemkabilan@rediffmail.com (S. Kabilan).

0022-2860/$ - see front matter Crown Copyright © 2010 Published by Elsevier B.V. All rights reserved.
doi:10.1016/j.molstruc.2010.02.005

2.4. Single crystal X-ray diffraction and computational detail

Single crystal X-ray data were collected using a Bruker Kappa CCD diffractometer with Mo Kα (λ = 0.71073 Å) at room temperature. Semi empirical absorption corrections were applied using SADABS program. The structure was solved using direct method and refined by full matrix least-squares method on F^2 with anisotropic thermal parameters for all non hydrogen atoms SHELXL-97 [10]. Hydrogen atoms bonded to the carbon atoms were placed in chemically acceptable position. The structures were drawn by ORTEP-3 [11] and Mercury [12] programs.

The molecular structure of compound **S10** in the ground state (in vacuum) is optimized by HF with 6-311++G(d,p) higher basis set. The calculation is performed using Gaussian 03 program [13] package on personal computer.

3. Results and discussion

3.1. Analytical data and IR spectral analysis

The reported new hydrazones (**S10**–**S23**) were synthesized as shown in Scheme 1 and their analytical data (Table 1) are agreed well with their proposed molecular formulae. The representative IR spectrum (compound **S11**) is given in Fig. 1. In IR spectra, the presence of C=N stretching frequency around 1640 and 1680 cm^{-1} confirm the hydrazone formation. In semicarbazones, the expected C=O absorption band should be merged with the band due to C=N stretching. A collection of bands observed in the region of 3196–3512 cm^{-1} are due to N–H stretching frequency of piperidine ring and hydrazone analogues while the absorption band in the region 3070–2800 cm^{-1} are ascribed to aromatic and aliphatic C–H stretching frequencies.

3.2. ^{1}H NMR analysis

In order to investigate the spectral assignments of reported hydrazones (**S10**–**S23**), we have chosen **S11** as the representative compound. Figs. 2–4 show ^{1}H NMR, ^{1}H–^{1}H COSY and NOESY spectrum of compound **S11** and Figs. 5 and 6 show the selected HOMO and NOE correlations of compound **S11** whereas Table 2 represents the correlated chemical shift values of ^{1}H–^{1}H COSY and NOESY spectra. In ^{1}H NMR, there are two signals appeared at 4.34 and 4.23 ppm (J = 2.60 and 1.88 Hz, respectively) corresponds to each one proton integral. Also, these two signals have HOMO correlation with signals at 2.45 and 2.83 ppm, respectively. Moreover, these two signals have strong NOE with multiplet at 7.52 ppm and singlet at 2.45 and 2.83 ppm. Therefore without ambiguity, these two signals are attributed to benzylic protons H-2 and H-4. However, signals at 2.45 and 2.83 ppm have weak HOMO correlation with benzylic protons (H-2 and H-4) and strong correlation with multiplet centered at 1.48 ppm. Hence, signals at 2.45 and 2.83 ppm should be due to bridgehead protons H-1 and H-5, respectively. Of these two signals, one is highly deshielded due to spatial interaction between the nitrogen of hydrazone analogue and one of the bridgehead proton (Fig. 7). Owing to this interaction, partial charges created between them. Consequently, the bridgehead α-carbon acquires slight negative charge and the attached proton gets slight positive charge as shown in Fig. 7. From this, the deshielded signal can be unambiguously assigned to *syn* α

Table 1
Analytical data for compounds (**S10**–**S23**).

Compound	R	R_1	R_2	Yield (%)	M.p. (°C)	M^+
S10	H	H	H	65	160	–
S11	H	H	F	60	196	399.89
S12	H	F	H	65	172	–
S13	H	H	Cl	67	202	–
S14	Cl	H	H	69	210	–
S15	H	H	Me	71	150	–
S16	H	H	OMe	85	133	–
S17	H	OMe	H	75	141	–
S18	H	H	H	92	205	347.58
S19	H	H	F	84	210	–
S20	H	F	H	81	136	–
S21	H	Cl	H	75	146	–
S22	Cl	H	H	77	226	–
S23	H	H	Me	73	134	–

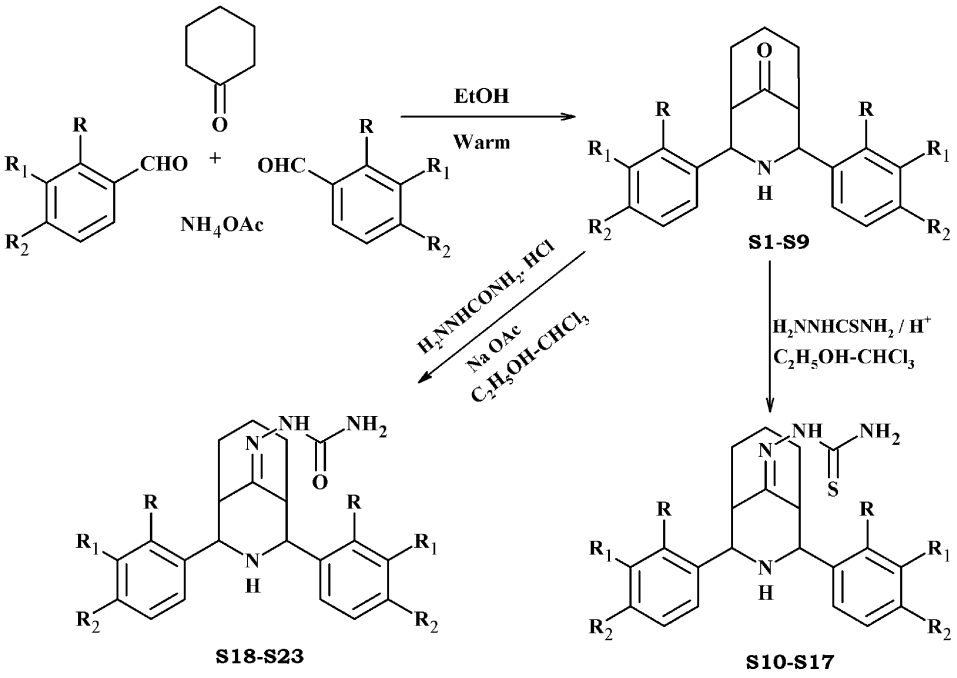

Scheme 1. Schematic diagram showing the synthesis of compounds **S10**–**S23**.

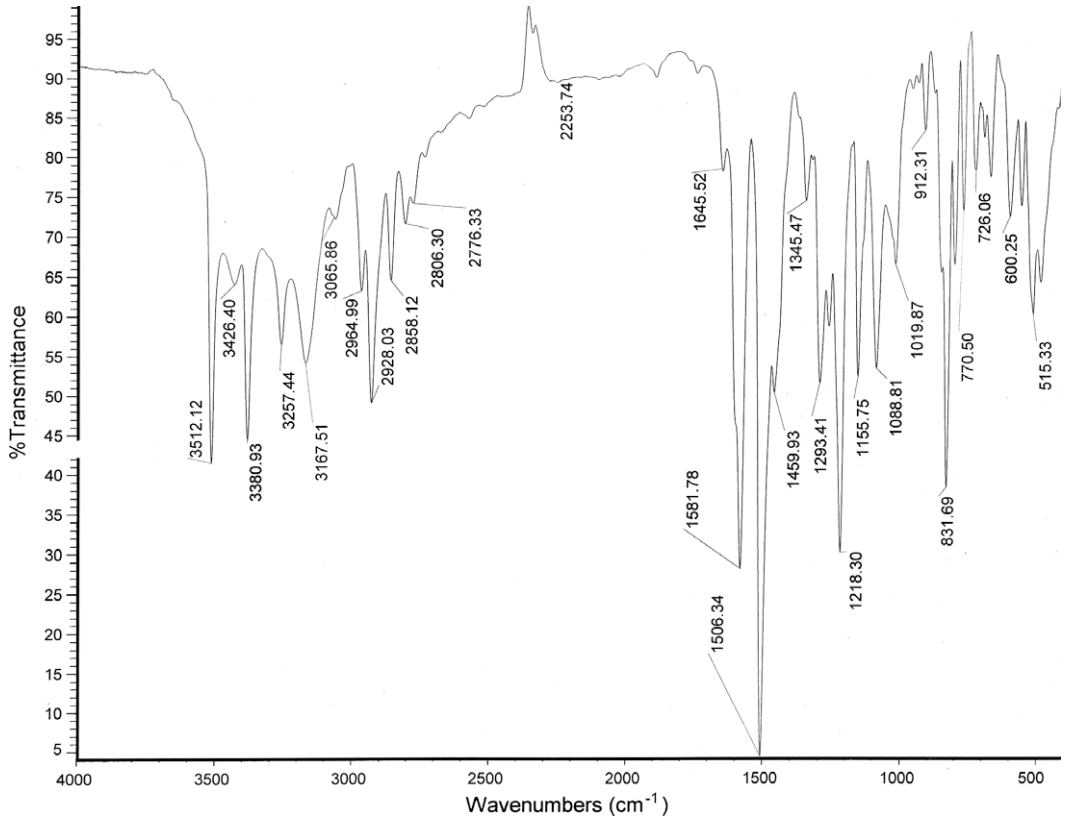

Fig. 1. IR spectrum of compound **S11**.

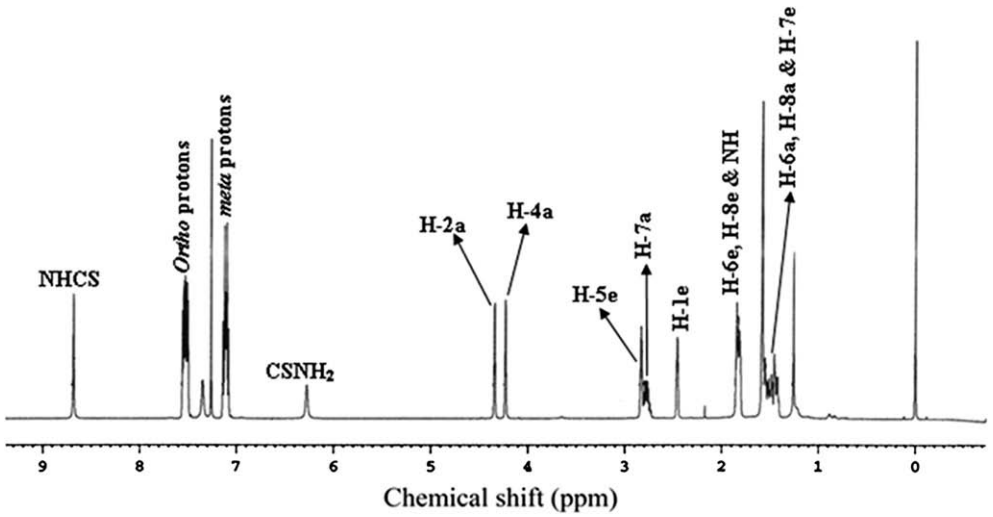

Fig. 2. ^{1}H NMR spectrum of compound **S11**.

(H-5) bridgehead proton whereas shielded signal is assigned to anti α (H-1) proton.

Three and two protons signal observed, respectively at 1.48 and 1.83 ppm which have strong HOMO correlation with bridgehead protons (H-1 and H-5) signal and the signal at 2.77 ppm. This indicates that these two signals should be due to methylene protons (C-6 and C-8). Among the said two signals (1.48 and 1.83 ppm) deshielded signal is assigned to H-6e and H-8e protons and the shielded one is assigned to H-6a and H-8a protons. The equatorial proton is highly deshielded than axial proton is due to the anisotropy of the C–C single bonds. Furthermore, the signal for H-7e proton is also be merged with H-6a/H-8a protons signal which substantiated by the integral values whereas the H-7a proton signal appeared at 2.77 ppm. Among the H-7a and H-7e protons signal, H-7a proton is deshielded due to deshielding effect exerted by the nitrogen lone pair and it creates vander Waals interaction. Due to this, C–H(7a) bond becomes polarized and as a consequence, carbon and the attached proton acquires negative and positive charges, respectively. Therefore, H-7a proton signal is highly deshielded than H-7e proton.

The benzylic protons (H-2 and H-4) have also shown a cross peak with multiplet at 7.51 ppm which suggests that the signal

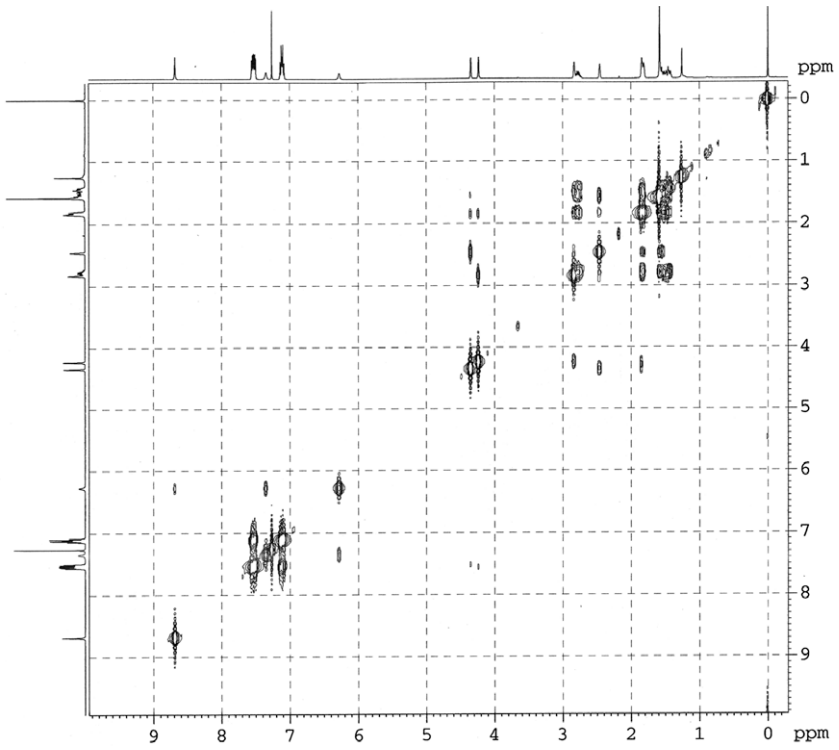

Fig. 3. $^{1}H–^{1}H$ COSY spectrum of compound **S11**.

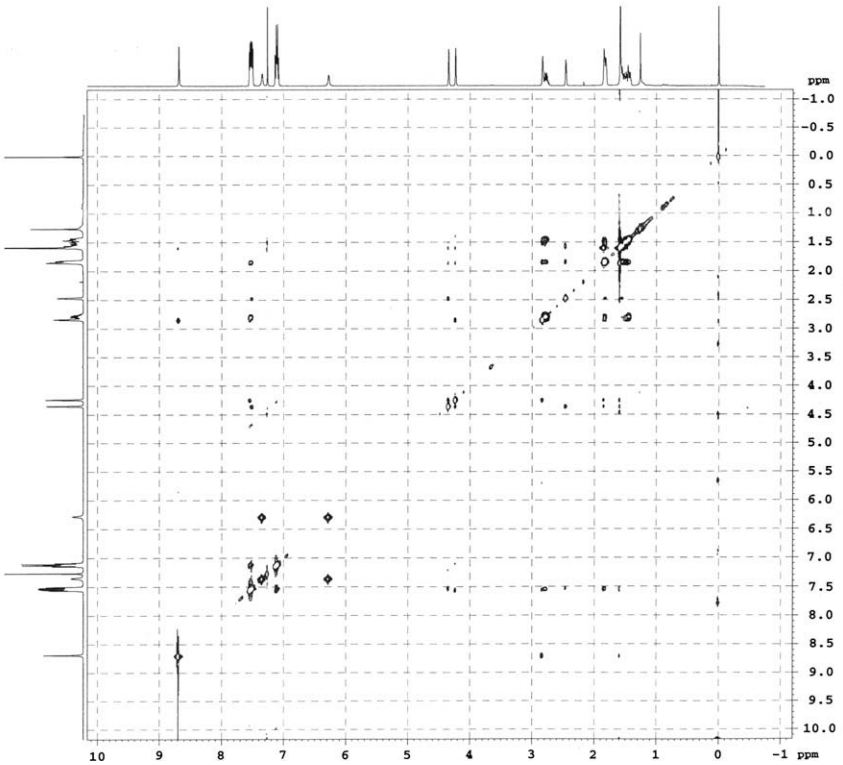

Fig. 4. NOESY spectrum of compound **S11**.

at 7.51 ppm with four protons integral is due to *ortho* protons (H-2″ and H-4″) of the phenyl groups. However, the *ortho* protons signal at 7.51 ppm has strong HOMO correlation with quartet centered at 7.10 ppm. Hence, the signal at 7.10 ppm is due to *meta* protons (H-2‴ and H-4‴) of the phenyl groups.

In thiosemicarbazone (**S10**–**S17**), the –NHCS and $–CSNH_2$ protons signal appeared around 8.8 and 6 ppm, respectively whereas in semicarbazones (**S18**–**S23**), the NHCO protons appeared around 8.8 ppm. But, the $–CONH_2$ protons are not appeared as singlet at 6 ppm with two protons integral as that $CSNH_2$ protons. Instead,

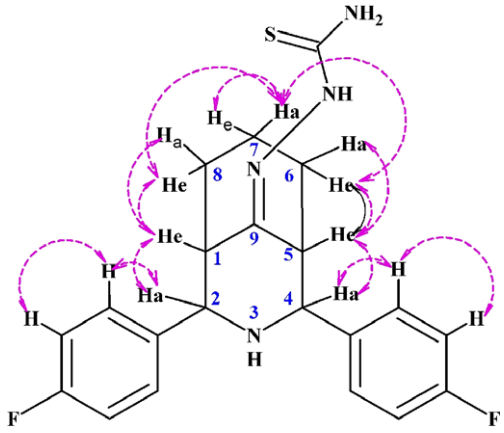

Fig. 5. ^{1}H–^{1}H COSY correlation of compound **S11**.

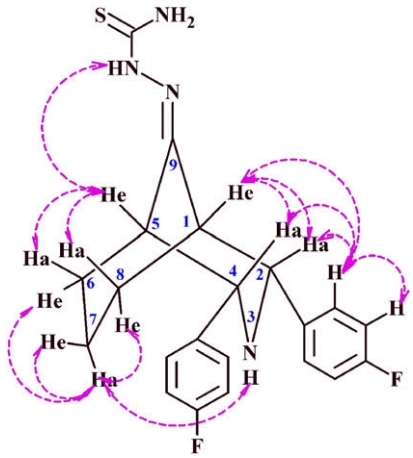

Fig. 6. NOESY correlation of compound **S11**.

Table 2
Selected ^{1}H–^{1}HCOSY and NOESY correlation chemical shifts of compound **S11**.

Signal	Correlations in HOMOCOSY	Correlations in NOESY
4.34 (d, 1H, H-2a)	1.83, 2.45, 7.51	1.51, 1.83, 2.45
4.23 (d, 1H, H-4a)	1.83, 7.51	1.51, 1.83, 2.83
2.83 (s, 1H, H-5e)	1.51, 1.83, 4.23	1.51, 1.83
2.45 (s, 1H, H-1e)	1.51, 1.83, 4.34	4.34, 7.51
2.77 (m, 1H, H-7a)	1.39, 1.83,	1.51, 1.83
7.51	7.10	1.51, 1.83, 2.45, 2.83, 4.23, 4.34

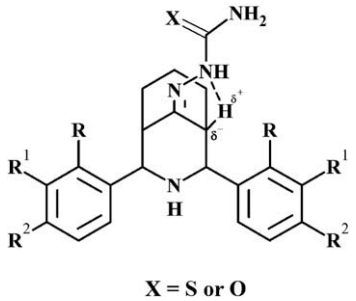

Fig. 7. CH(5e)–NH bond interaction.

there are two broad singlets appeared in the region of 4–6 ppm. The observed broad singlet is due to restricted rotation about the NCO bond in NMR time scale. In addition, the presence of NCO bond in semicarbazone analogue may lead to existence of different amide conformers. In order to study the amide conformation in **S18**–**S23**, NH_2 protons are designated as H_a and H_b as shown in Fig. 8. Fig. 8a–8d provides the appropriate amide conformation of semicarbazone compounds. Of the Fig. 8a–8d, the cis form (Fig. 8c and 8d) is more stable due to their intramolecular hydrogen bonding between $N_{(1)}$ and $N_{(a)}$ or $N_{(1)}$ and $N_{(b)}$. Table 3 contains the proton chemical shifts of compounds **S10**–**S23**.

3.3. ^{13}C NMR analysis

The representative ^{13}C NMR spectrum (compound **S11**) is depicted in Fig. 9 and the chemical shifts of compounds **S10**–**S23** are given in Table 4. Assignment of both piperidine and cyclohexane ring carbon signals were assigned by comparing the parent ketones. However, in compounds **S11**, **S12**, **S19** and **S20**, two signals observed around 163 and 161 ppm are due to fluorine attached ipso carbons. The observed two signals are due to C–F coupling between carbon and attached fluorine atom. Similarly another pair of signal observed for all hydrazones in the region 133–140 ppm are assigned to C-2′ and C-4′ ipso carbons.

For thiosemicarbazones (**S10**–**S17**), the C=S and C=N carbons signal appeared around 175 and 159 ppm, respectively whereas in semicarbazone compounds (**S18**–**S23**), the C=O/C=N carbon signals show around 158 ppm. For both the hydrazones, the ring carbon signals observed identically. However, there are two signals around 64 and 63 ppm are conveniently assigned to C-2 and C-4 carbons, respectively. Whereas, the bridgehead carbons C-1 and C-5 appeared around 46 and 39 ppm, respectively except compounds **S14** and **S22**. Interestingly, C-5 carbon signal shielded by 7 ppm due to spatial interaction between C-5 proton and lone pair nitrogen in hydrazone analogue. This interaction induces a polarity on the *syn* α C–H(e) bond so that the *syn* α-equatorial proton (H-5e) gets slight positive charge and the C-5 carbon gets slight negative charge as shown in Fig. 7. Consequently, the proton is deshielded and carbon is shielded. Therefore, the deshielded signal is assigned to C-1 carbon and shielded signal is assigned to C-5 car-

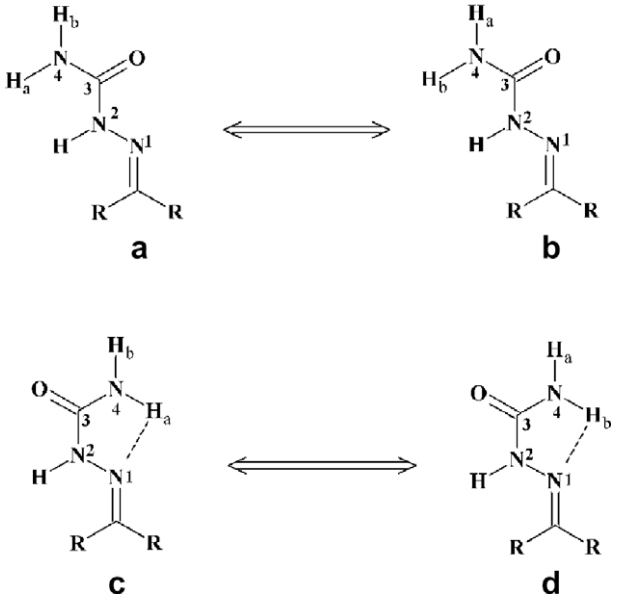

Fig. 8. The possible hydrazone analogue conformations.

Table 3
1H NMR Chemical shifts of compounds **S10**–**S23** [$\Delta\delta$ (ppm)].

Compound	H-2a (d)	H-4a (d)	H-1e (s)	H-5e (s)	H-7a (m)	H-6e, H-8e and NH (dd)	H-6a and H-8a	H-7e	CH_3/ OCH_3	NHCS (s)	$CSNH_2$/ $CONH_2$ (s)	Aromatic protons
S10	4.36	4.26 (s)	2.5	2.97	2.83	1.84	1.40–1.58 (m)		–	8.92	6.5	7.26–7.57 (m)
S11	4.34	4.24	2.46	2.85	2.77	1.83 (m)	1.41–1.58 (m)		–	8.75	6.32	7.11–7.50
S12	4.36	4.26	2.51	2.9	2.75	1.82	1.54 (m)	1.43 (m)	–	8.87	6.39	6.99–7.42 (m)
S13	4.34	4.23	2.47	2.88	2.75	1.8	1.53 (m)	1.43 (quintet)	–	8.85	6.38	7.50, (q); 7.39 (t)
S14	4.76	4.66	2.81 (m)	3.22 (d)	2.81	1.76	1.50–1.60 (m)	1.42 (quintet)	–	8.71	6.28	7.99 (t); 7.25–7.44
S15	4.31	4.2	2.45	2.88 (m)	2.8	1.84	1.50 (m)	1.38 (quintet)	2.37 (s)	8.88	6.44	7.22 (q); 7.44 (q)
S16	4.32	4.26	2.5	2.91	2.81	1.86	1.38–1.58 (m)		3.85 (d)	8.84	6.34	6.94 (q); 7.47 (q)
S17	4.29	4.18 (s)	2.43	2.82	2.8	1.87	1.47 (m)		3.83 (d)	8.74	6.33	6.83–7.36 (m)
S18	4.38	4.25	2.85	2.49	2.85	1.81 (m)	1.47		–	7.94	4.8 6.25	7.31–7.44 (m)
S19	4.35	4.26	3	2.45	2.74	1.73 (m)	1.48 (m)	1.71 (q)	–	8.8	5.00 6.30	7.07–7.62 (m)
S20	4.38	4.3	3.04	2.51	2.71	1.76–1.85 (m)	1.43 (m)	1.41 (quintet)	–	8.87	4.90 6.20	7.00–7078 (m)
S21	4.35	4.29	3.23	2.49	2.68	1.74 (m)	1.46–1.59 (m)	1.41 (quintet)	–	9.54	4.99 6.25	7.28–7.79 (m)
S22	4.77 (d)	4.65 (d)	3.12	2.80 (m)		1.71–1.75 (dd)	1.50–1.64 (m)	1.40 (quintet)	–	7.65	4.90 6.15	7.23–8.00 (m)
S23	4.33	4.21	2.8	2.46	2.80 (s)	1.82 (dd)	1.44 (m)		2.37	7.88	4.90 6.20	7.21 (q); 7.47(q)

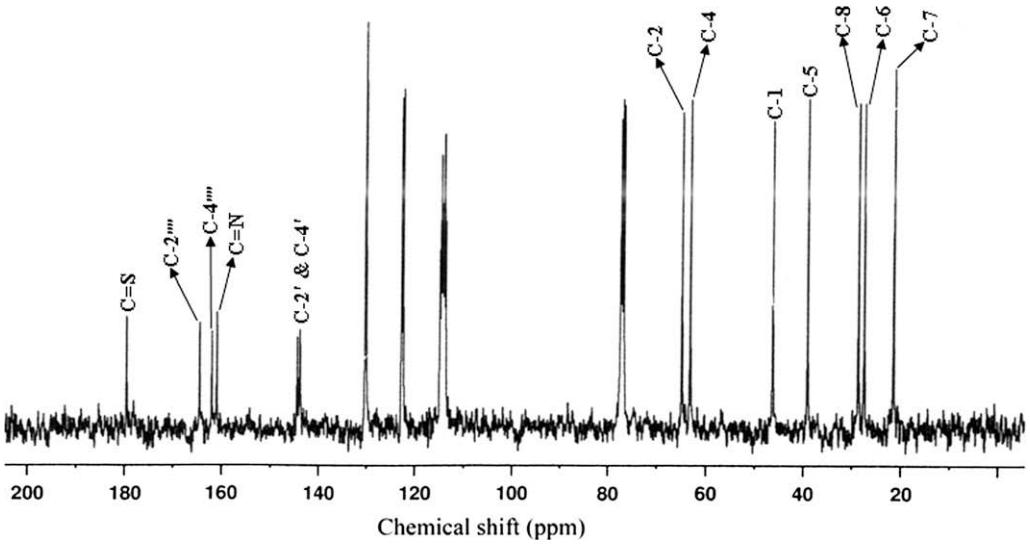

Fig. 9. ^{13}C NMR spectrum of compound **S11**.

bon. For compounds **S14** and **S22**, the benzylic and bridgehead carbons signal appeared around 61/60 and 41/34 ppm, respectively. This is due to van der Waals interaction between chlorine and benzylic/bridgehead protons (Fig. 10).

The ring methylene carbon signals C-6, C-7 and C-8 of cyclohexane are observed around 26, 21 and 28 ppm, respectively. Among the three carbon signals, C-7 carbon is shielded by about 7 ppm than C-6 and C-8. As stated earlier, this is due to van der Waals interaction between axial proton of C-7 carbon and lone pair nitrogen in piperidine ring. Owing to this interaction, C-7(H-a) bond becomes polarized. As a result, the proton acquires slight positive charge and carbon acquires slight negative charge. Therefore, the C-5 carbon is shielded and the proton is deshielded.

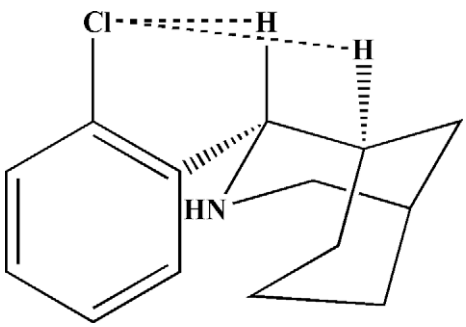

Fig. 10. Interaction between the Cl at ortho position and benzylic/bridge-head protons.

Table 4
^{13}C NMR Chemical shifts of compounds **S10**–**S23** [$\Delta\delta$ (ppm)].

Compound	C-1	C-2	C-4	C-5	C-6	C-7	C-8	C-9	C=S/ C=O	C-2′	C-4′	Other aryl carbons
S10	46.40	65.38	63.79	39.14	27.39	21.46	28.64	161.89	179.13	141.89	141.32	126.86, 127.10, 127.50, 127.82, 128.52, 128.65
S11	46.29	64.72	63.10	39.06	27.25	21.38	28.46	161.29	179.12	137.37	136.83	163.50, 160.91, 136.83, 115.08, 115.48, 115.28 128.61,128.35
S12	46.28	64.84	63.16	39.05	27.40	21.38	28.59	160.95	179.59	144.43	143.85	164.40, 161.96 130.15, 122.72, 122.39, 114.85, 114.60, 114.35, 114.20, 113.93, 113.69
S13	46.29	64.90	63.22	39.03	27.29	21.39	28.49	160.92	179.37	140.20	139.65	133.750, 133.431, 128.90, 128.81, 128.44, 128.166
S14	42.17	62.32	60.60	34.94	27.18	21.00	28.48	160.12	179.38	138.77	138.14	132.85, 130.08, 128.93, 128.65, 126.91
S15	46.55	65.30	63.62	39.34	27.37	21.43	28.59	162.35	179.38	139.00	138.44	137.32, 137.01, 129.22, 129.14, 126.95, 126.72
S16	46.34	65.10	63.48	39.12	27.50	21.34	28.70	161.99	178.98	143.58	143.01	158.87, 159.07, 128.88, 127.88, 113.92, 113.80
S17	46.51	64.90	63.30	39.26	27.33	21.48	28.56	162.26	179.03	134.03	133.44	129.56, 129.45, 119.41, 119.16, 113.08, 112.92, 112.65, 112.23
S18	46.33	65.07	63.57	38.52	26.90	21.49	28.24	158.35		142.44	142.07	126.32, 126.87, 127.13, 127.26, 127.42, 128.41
S19	46.40	65.11	63.04	38.55	26.81	21.47	28.13	158.53		138.05	137.72	164.28, 163.43, 137.72, 115.41, 115.20
S20	46.08	65.00	62.77	38.21	26.83	21.34	28.11	158.24		145.07	144.82	163.52, 161.82 129.97, 129.88, 129.82, 129.74, 128.30, 122.44, 114.50, 114.26, 114.05, 113.89, 113.67
S21	46.17	65.27	62.93	38.24	26.85	21.41	28.08	157.98		144.52	144.28	129.67, 127.55, 127.06, 125.04
S22	41.99	61.97	60.20	34.19	26.97	21.08	28.38	156.84		139.04	138.46	129.99, 129.92, 128.72, 128.67, 128.46, 128.31, 126.94, 126.81
S23	46.37	65.33	63.42	38.61	26.90	21.52	28.25	158.18		137.05	136.84	139.45, 139.04 126.77, 126.99, 128.31, 129.06, 129.11

3.4. Stereochemistry and conformational analysis

In order to understand the conformational analysis of piperidine and cyclohexane rings, vicinal coupling constants are more important parameter. However, the present set of hydrazones, coupling constants values could not be resolved well because all the signals appeared as singlet and multiplet except benzylic protons. Therefore, conformation of two six membered rings were successfully achieved with the help of chemical shift parameters, single crystal X-ray analysis and semi empirical calculation. However, the obtained vicinal couplings constants of J_{2a1e} and J_{4a5e} values around 2 Hz suggest that axial–equatorial couplings. Therefore, benzylic and bridgehead protons occupy axial and equatorial orientations, respectively. Besides, the strong NOEs between H-1 and H-2 and also between H-1 and H-4 clearly confirm that the benzylic and bridgehead protons are occupying axial and equatorial dispositions, respectively. Similarly, the H-7a proton has strong NOE with H-7e proton and its adjacent equatorial protons. This NOE states that the signal at 1.83 ppm is due to equatorial protons. Besides, the NOE between NH proton in hydrazone analogue and H-5 bridgehead proton clearly reveals that the H-5 proton is *syn* to the hydrazone analogue. From the chemical shifts, coupling constants and NOE analysis, the compounds (**S10**–**S23**) may adopt twin-chair conformations. This is further confirmed by the single crystal X-ray analysis.

3.5. Crystal structure and theoretical analysis

Table 5 gives crystal data, data collection, and refinement parameters of compound **S18** whereas Table 6 shows the selected bond lengths and angles of non hydrogen atoms. Fig. 11 shows the ORTEP diagram of the compound **S18** with 30% probability level. The asymmetric unit contains two crystallographically independent molecules (A and B). The bond distances between C21–O1 and C21–N4 are less than that of the standard values. This may be due to the partial double bond character between C21 and O1 and C21 and N4.

Table 5
Crystal data and structure refinement parameters for **S18**.

Empirical formula	$C_{21}H_{24}N_4O$
Formula weight	348.44
Wavelength (Å)	0.71073
Crystal system, space group	Triclinic, $P\bar{1}$
Cell dimensions	
a (Å)	10.2564(2)
b (Å)	12.1453(3)
c (Å)	15.4442(4)
α (°)	90
β (°)	92
γ (°)	101
Z	4
D_{calc} (g/cm^3)	1.227
Volume (Å^3)	1886.50(8)
θ Range for data collection (°)	1.32–28.31
F(0 0 0)	744
Index range	$-13 \leqslant h \leqslant 10$, $-16 \leqslant k \leqslant 16$, $-20 \leqslant l \leqslant 20$
Number of parameters	501
Absorption correction	None
Goodness-of-fit	0.997
Largest diff. peak and hole (e Å^{-3})	0.180 and −0.143
Data/restraints/parameters	8630/0/501
Refinement method	Full-matrix least-squares on F^2 (SHELXL-97)

Table 6
Geometric parameters of compound **S18**.

Atoms	Length	Atoms	Length
C(1)–C(5)	1.496(2)	C(3)–C(4)	1.542(2)
C(1)–C(6)	1.541(2)	C(4)–C(5)	1.504(2)
C(1)–C(2)	1.543(2)	C(4)–C(8)	1.542(3)
C(1)–H(1)	0.9800(1)	C(6)–C(7)	1.529(2)
C(2)–N(1)	1.465(2)	C(7)–C(8)	1.518(3)
C(2)–C(9)	1.516(2)	C(21)–O(1)	1.229(2)
C(3)–N(1)	1.459(2)	C(21)–N(4)	1.347(2)
C(3)–C(15)	1.518(2)	C(21)–N(3)	1.351(2)
N(2)–N(3)	1.3875(19)		
Atoms	**Angle**	**Atoms**	**Angle**
C(5)–C(1)–C(6)	107.19(14)	N(2)–C(5)–C(1)	119.10(14)
C(5)–C(1)–C(2)	108.95(14)	N(2)–C(5)–C(4)	129.22(15)
C(6)–C(1)–C(2)	115.10(14)	C(1)–C(5)–C(4)	111.53(13)
N(1)–C(2)–C(9)	110.49(13)	C(7)–C(6)–C(1)	113.66(14)
N(1)–C(2)–C(1)	109.99(13)	C(8)–C(7)–C(6)	112.71(16)
C(9)–C(2)–C(1)	112.43(14)	C(7)–C(8)–C(4)	114.00(14)
N(1)–C(3)–C(15)	111.69(13)	C(10)–C(9)–C(14)	117.70(16)
N(1)–C(3)–C(4)	110.79(13)	C(10)–C(9)–C(2)	120.33(14)
C(15)–C(3)–C(4)	110.29(13)	C(14)–C(9)–C(2)	121.96(15)
C(5)–C(4)–C(8)	107.10(14)	O(1)–C(21)–N(4)	123.25(16)
C(5)–C(4)–C(3)	107.96(13)	O(1)–C(21)–N(3)	120.61(16)
C(8)–C(4)–C(3)	115.20(13)	N(4)–C(21)–N(3)	116.10(17)

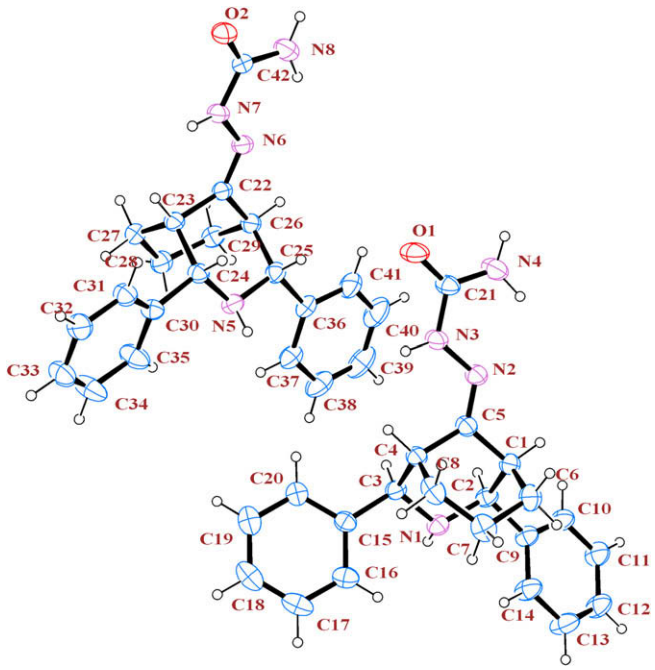

Fig. 11. ORTEP diagram of compound **S18**.

Table 7
Optimized geometrical parameters of compound **S10**.

Interatomic distances (Å)			
C1–C4	1.460	C4–C50	1.302
C1–N48	1.494	C10–C15	1.613
C1–C29	1.539	C12–C15	1.705
C2–C3	1.609	C40–C42	1.470
C2–C18	1.541	C40–N44	1.469
C2–N48	1.584	C40–O47	1.566
C3–C12	1.603	N41–C50	1.293
C3–C50	1.349	N41–N42	1.400
Bond angle (°)			
C1–C4–C50	105.02	C10–C4–C50	91.88
C2–C3–C50	83.07	C12–C3–C50	109.58
C2–C3–N48	112.62	N42–N41–C50	120.46
C3–C2–N48	112.62	N42–C40–N44	120.10
C3–C50–C4	130.06	N42–C40–O47	119.92
C4–C1–N48	100.31	C44–C40–O47	119.97
C4–C1–C29	113.31	N48–C2–C18	106.27
C10–C15–C12	113.96	N48–C1–C29	114.90
Torsion angle (°)			
C1–N48–C2–C3	58.17	C15–C10–C4–C50	–41.70
C2–N48–C1–C4	–50.80	C30–C29–C1–N48	–92.25
C3–C2–C18–C19	–88.82	N48–C2–C3–C50	–51.90
C3–C12–C15–C10	–56.51	N48–C1–C4–C50	52.26
C4–C10–C15–C12	48.43		

In the conformational analysis of compound **S18**, six membered heterocyclic piperidine ring adopts normal chair conformation with the puckering parameters [14] being q_2 and q_3 are 0.045 Å and 0.5773 Å, respectively. The total puckering amplitude, Q_T = 0.5791 Å; θ = 4.46°. Similarly, cyclohexane ring also adopts normal chair conformation with puckering parameters being q_2 and q_3 are 0.136 Å and 0.559 Å, respectively. Q_T = 0.575 (2) Å, θ = 13.73°. In both the molecules, phenyl rings occupy equatorial orientations. The packing of the molecule in the crystal lattice is given in Fig. 12 which shows that compound **S18** is stabilized by strong intermolecular N–H···O hydrogen bonding of 2.89 (2) Å.

The optimized structural parameters (bond lengths, bond angles and dihedral angles) for thermodynamically preferred geometry of compound **S10** determined by HF level with 6-311G(d,p) basis set are listed in Table 7, with the atom numbering scheme of the molecule is shown in Fig. 13. As given in Table 7, most of the optimized bond lengths and bond angles are slightly overestimated as well as underestimated, because the molecular states are

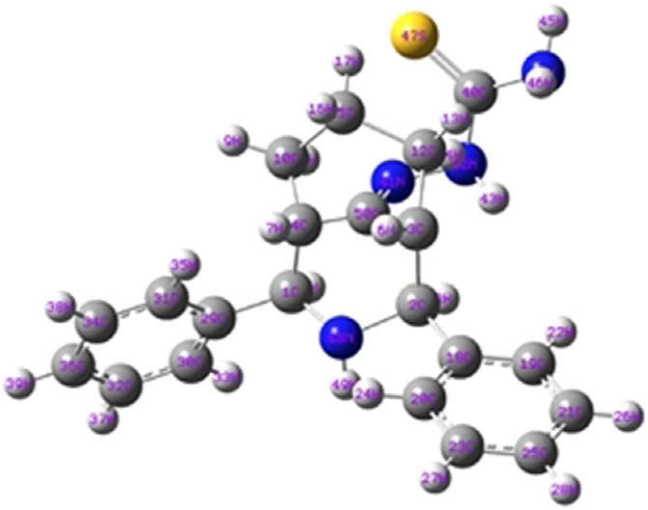

Fig. 13. Optimized structure of compound **S10**.

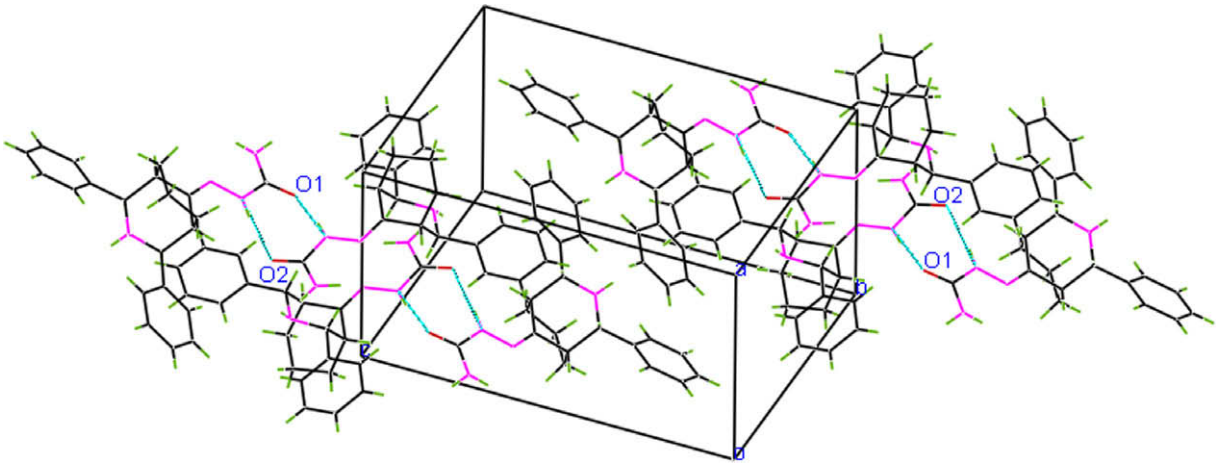

Fig. 12. Packing diagram of compound **S18**.

different during experimental and theoretical process. One isolated molecule is considered in gas phase during theoretical calculation, while many packing molecules are treated in condensed phase during the experimental measurement. However, the ring part of optimized parameters of the molecule shows good agreement with X-ray data [15]. Piperidine and cyclohexane ring moieties are essentially adopt chair conformation as evident from the torsional angles [N48–C1–C4–C50 = 52.26° and C15–C10–C4–C50 = −41.70°]. In the molecular optimized structure, the hydrazone analogue is *syn* to C3 bridgehead proton as confirmed by the torsion angle C3–C50–N41–N42 = −1.19°.

4. Conclusion

All the synthesized 2,4-diaryl-3-azabicyclo[3.3.1]nonan-9-one hydrazones (**S10**–**S23**) were characterized by analytical and spectral (^{1}H NMR, ^{13}C NMR, HOMOCOSY and NOESY) methods. Besides, the single crystal X-ray diffraction analysis was studied for compound (**S18**) whereas the molecular optimization geometry was carried out for compound **S10**. From the chemical shifts, coupling constants and single crystal X-ray analysis, the title hydrazones were found to adopt twin-chair conformations with equatorial orientation of the aryl groups.

Supplementary materials

NMR and IR data for other investigated compounds can be obtained on personal demand from authors. Crystallographic data for the structural analysis have been deposited with the Cambridge Crystallographic Data Centre, CCDC-698833. Copy of this information may be obtained free of charge from The Director, CCDC, 12 Union Road, Cambridge CB2 1EZ, UK (Fax: +44 1223 336033; e-mail: deposit@ccdc.cam.ac.uk or http://www.ccdc.cam.ac.uk).

Acknowledgements

Authors are thankful to NMR Research Centre, IISc, Bangalore for recording NMR and Department of Chemistry, Indian Institute of Technology, Madras, for recording single crystal X-ray data collection.

References

[1] H. Beraldo, Quim. Nova 27 (2004) 461.
[2] D.L. Klayman, J.F. Bartosevich, T.S. Griffin, C.J. Mason, J.P. Scovill, J. Med. Chem. 22 (1979) 855.
[3] X. Du, C. Guo, E. Hansell, P.S. Doyle, C.R. Caffrey, T.P. Holler, J.H. McKerrow, F.E. Cohen, J. Med. Chem. 45 (2002) 2695.
[4] I. Chiyanzu, E. Hansell, J. Gut, P.J. Rosenthal, J.H. McKerrow, K. Chibale, Bioorg. Med. Chem. Lett. 13 (2003) 3527.
[5] D.C. Greenbaum, Z. Mackey, E. Hansell, P. Doyle, J. Gut, C.R. Caffrey, J. Lehrman, P.J. Rosenthal, J.H. McKerrow, K. Chibale, J. Med. Chem. 47 (2004) 3212.
[6] N. Fujii, J.P. Mallari, E.J. Hansell, Z. Mackey, P. Doyle, Y.M. Zhou, J. Gut, P.J. Rosenthal, J.H. McKerrow, R.K. Guy, Bioorg. Med. Chem. Lett. 15 (2005) 121.
[7] Z.I. Cabantchik, S. Moody-Haupt, V.R. Gordeuk, FEMS Immunol. Med. Microbiol. 26 (1999) 289.
[8] D.R. Richardson, Exp. Opin. Invest. Drugs 8 (1999) 2141.
[9] P. Parthiban, R. Ramachandran, G. Aridoss, S. Kabilan, Magn. Reson. Chem. 46 (2008) 780;
P. Parthiban, S. Balasubramanian, G. Aridoss, S. Kabilan, Spectrachim. Acta Part A 70 (2008) 11;
G. Aridoss, S. Balasubramanian, P. Parthiban, S. Kabilan, Spectrochim. Acta Part A 68A (2007) 1153.
[10] G.M. Sheldrick, SHELXS-97 and SHELXL-97, Software for crystal structure analysis, Siements analytical X-ray instruments Inc., Madison, WI, 1997.
[11] L.J. Farrugia, J. Appl. Crystallogr. 30 (1997) 565.
[12] I.J. Bruno, J.C. Cole, P.R. Edgington, M.K. Kessler, C.F. Macrae, P. McCabe, J. Pearson, R. Taylor, Acta Crystallogr. B58 (2002) 389.
[13] M.J. Frisch, G.W. Trucks, H.B. Schlegel, G.E. Scuseria, M.A. Robb, J.R. Cheeseman, J.A. Montgomery Jr., T. Vreven, K.N. Kudin, J.C. Burant, J.M. Millam, S.S. Iyengar, J. Tomasi, V. Barone, B. Mennucci, M. Cossi, G. Scalmani, N. Rega, G.A. Petersson, H. Nakatsuji, M. Hada, M. Ehara, K. Toyota, R. Fukuda, J. Hasegawa, M. Ishida, T. Nakajima, Y. Honda, O. Kitao, H. Nakai, M. Klene, X. Li, J.E. Knox, H.P. Hratchian, J.B. Cross, C. Adamo, J. Jaramillo, R. Gomperts, R.E. Stratmann, O. Yazyev, A.J. Austin, R. Cammi, C. Pomelli, J.W. Ochterski, P.Y. Ayala, K. Morokuma, G.A. Voth, P. Salvador, J.J. Dannenberg, V.G. Zakrzewski, S. Dapprich, A.D. Daniels, M.C. Strain, O. Farkas, D.K. Malick, A.D. Rabuck, K. Raghavachari, J.B. Foresman, J.V. Ortiz, Q. Cui, A.G. Baboul, S. Clifford, J. Cioslowski, B.B. Stefanov, G. Liu, A. Liashenko, P. Piskorz, I. Komaromi, R.L. Martin, D.J. Fox, T. Keith, M.A. Al-Laham, C.Y. Peng, A. Nanayakkara, M. Challacombe, P.M.W. Gill, B. Johnson, W. Chen, M.W. Wong, C. Gonzalez, J.A. Pople, Gaussian, Inc., Wallingford, CT, 2004.
[14] D. Cremer, J.A. Pople, J. Am. Chem. Soc. 97 (1975) 1354.
[15] N. Sampath, S.M. Malathy Sony, M.N. Ponnuswamy, M. Nethaji, Cryst. Res. Technol. 39 (2004) 821.